ADVANCED OPTICAL MATERIALS
www.advopticalmat.de

Multidirectional Light-Harvesting Enhancement in Dye Solar Cells by Surface Patterning

*Carmen López-López, Silvia Colodrero, Alberto Jiménez-Solano, Gabriel Lozano, Reyes Ortiz, Mauricio E. Calvo, and Hernán Míguez**

One dimensional gratings patterned on the surface of nanocrystalline titania electrodes are used as a light harvesting strategy to improve the overall performance of dye solar cells under both frontal and rear illumination conditions. A soft-lithography-based micromoulding approach is employed to replicate a periodic surface relief pattern onto the surface of the electrode, which is later sensitized with a dye. As the patterned surface acts as an optical grating both in reflection and transmission modes, its effect is to increase the light path of diffracted beams within the absorbing layer when it is irradiated either from the electrode or the counter electrode for a broad range of angles of incidence on each surface. Full optical and photovoltaic characterization demonstrates not only the optical quality of the patterned surfaces but also the multidirectional character of the enhancement of light harvesting and conversion efficiency. The approach herein presented thus permits to preserve the operation of the cell when irradiated from its two faces while increasing its overall power conversion efficiency. This feature is a key advantage over other light harvesting efficiency enhancing methods, such as the deposition of a back diffuse scattering layer, in which the performance of the cell under illumination from one of its sides is enlarged at the expense of reducing the output under reverse irradiation conditions.

1. Introduction

Thin film photovoltaic technologies, such as dye solar cells (DSCs),[1,2] have attracted considerable interest due to their potential as low-cost energy sources. However the need to use thin photoactive layers leads to poor optical absorption restricting the performance of the device. To address this problem, a number of photon management techniques have been proposed and realized in order to enlarge the time of residence of targeted photons into the absorbing layer. Although many different nanostructures have been employed for this purpose in other types of thin film solar cells,[3–7] their integration in DSCs has been delayed until recently as a result of the difficulties that arise when optical materials are combined with the usually employed TiO_2 (anatase) pastes and corrosive electrolytes used in DSCs. The design of materials ad hoc has allowed overcoming these obstacles and high expectations are now being put on them. Conventionally, large anatase particles acting as scattering centres[8–10] have been employed to trap freely propagating photons into the photoanode by multiple scattering. This optical phenomenon gives rise to a large enhancement of the light harvesting efficiency, but also implies that the DSC turns opaque. Motivated originally by the possibility to take advantage of slow photon effects, and later by that of preserving transparency in cells of enhanced efficiency, different periodic architectures with photonic crystal properties have been proposed.[11–14] In this case, the primary mechanism of improvement is the back reflection of light frequencies that falls within the photonic band gap, although different types of optical resonances have been shown to contribute to the enhancement as well.[15,16] In all these approaches, as they are based on diffuse or specular back reflection, the improvement of performance when light reaches the cell from the front side is inevitably accompanied by a decrease of the efficiency when light comes from the counter electrode. As an alternative to these approaches, very recently, relief patterns have been moulded onto the surface of nanocrystalline anatase films with the aim of diffracting unabsorbed light back into the electrode with an oblique angle. Initially reported results prove the potential of this approach to largely increase the light harvesting efficiency without adding any extra layer to the cell.[17–20] Besides, these results indicate that it should be possible to improve efficiency while preserving the multidirectional operation of the cell (i.e., under front and rear illumination conditions), as the nanostructured surface of a transparent material behave as diffracting interface and, hence, as potential absorption enhancer at any angle of incidence of light on its surface.

In this work, we demonstrate that surface relief patterns can be used as multidirectional enhancers of the efficiency of DSC. We used a combination of soft-lithography and micro-stamping

Dr. C. López-López, Dr. S. Colodrero, A. Jiménez-Solano, Dr. G. Lozano, R. Ortiz, Dr. M. E. Calvo, Prof. H. Míguez
Multifunctional Optical Materials Group
Instituto de Ciencia de Materiales de Sevilla
Consejo Superior de Investigaciones Científicas-Universidad de Sevilla(US-CSIC)
Américo Vespucio 49 41092, Sevilla, Spain
E-mail: h.miguez@csic.es

DOI: 10.1002/adom.201400160

techniques to replicate the structure of a one dimensional optical grating onto the surface of a film of nanocrystalline titania deposited on a conducting glass. In this way, the interface between the electrode and the electrolyte in the cell becomes highly diffractive. Such interface works as an optical grating in both reflection and transmission modes, and it is therefore capable of enlarging the time of residence of photons in the absorbing electrode regardless of their direction of incidence on the cell. We provide evidence of multidirectional enhanced photovoltaic performance by measuring the cell power conversion efficiency when light impinges on the cell from both the electrode and the counter electrode sides, and for a wide range of incident angles in each case. Our results are of interest for applications in photovoltaic window panes that should be able of capturing light from both outdoors and indoors.

2. Results and Discussions

The structural quality of the nanopatterned replicas was analyzed by atomic force microscopy (AFM). **Figure 1** displays the images attained as well as the profiles extracted along directions perpendicular to the grooves for the h-PDMS, Figure 1A, and the nanocrystalline titania electrode replicas, Figure 1B. In both cases, the period and the asymmetric shape of the blazed grating is preserved, although the average depth of the groove in the TiO_2 electrode is smaller than in the original master (135 nm versus the 180 nm average depth of the mold). Moreover, the roughness of the nanocrystalline titania film increases. This is likely a result of the less conformal coupling between the nanocrystalline paste and the polymer replica, and of the high temperature sintering process at which the film is subjected to mechanically stabilize it. The period of the grating (833 nm) was elected to yield diffraction effects at frequencies matching the absorption band of the dye that was used to sensitize the porous electrode, i.e., a ruthenium based dye (N-719). We chose

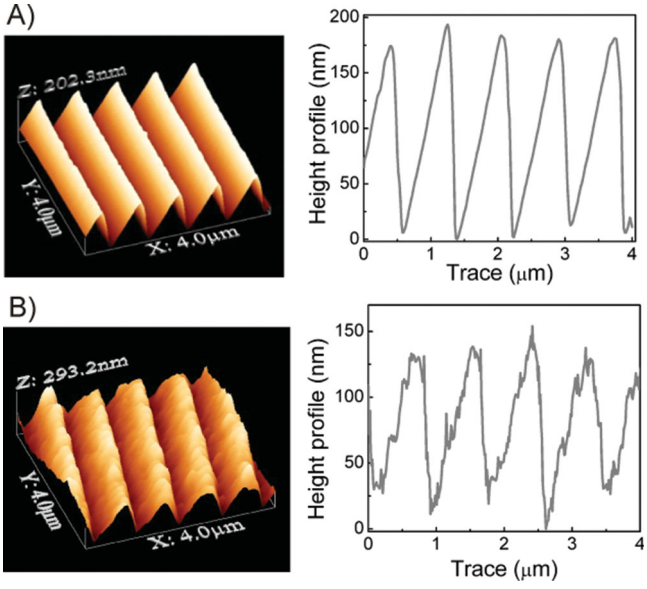

Figure 1. AFM images (left) cross sectional analysis (right) of (A) elastomeric stamp and (B) nc-TiO_2 patterned electrode.

to use an asymmetric relief because the added intensity of its first diffraction orders (m = 1 and m = –1) is larger than that of the first diffraction orders of a symmetric grating. First diffraction orders are expected to be more robust against structural imperfections that may arise during the replication process, so we decided to use a grating with a profile that maximized the amount of energy carried in those lower order modes. In Figure S1 of the supporting information we include the theoretical diffraction intensity spectrum of zero and first order modes for both symmetric and asymmetric triangular gratings, which were employed to justify our choice. On the other hand, the asymmetry of the pattern employed should also be observed in the dependence of the photovoltaic response with the angle of incidence, which will further confirm the origin of the enhancement effects herein described.

The light diffraction properties of the patterned nanocrystalline electrodes were confirmed by analysing their behaviour upon impinging a light beam on the surface. The intensity of diffracted light was analysed for beams of different colour. Results are summarized in **Figure 2**, in which a picture illustrates the pattern of diffraction spots observed when four different beams impinge simultaneously on the electrode (Figure 2A). Also, the intensity of reflected beams vs. wavelength and diffraction angle is plotted in Figure 2.B. The grating equation that determines the angle of diffraction for a given wavelength λ, is:[21]

$$m\lambda = d(\sin\theta_i + \sin\theta_r) \quad (1)$$

where d is the groove spacing, m is the diffraction order, and θ_i and θ_r are the incidence and reflected diffraction angles measured from the grating normal, respectively. In our case d = 833 nm and the first diffraction orders (m = 1 and m = –1) are studied for an incident angle $\theta_i = 0°$. The different response of the patterned electrode at right or left angles results from the asymmetric shape that the surface relief features in the grating. In fact, the blaze determines that modes labeled as m = –1 carry more energy than those reflected at the other side of the normal. In order to assess the optical quality of the gratings replicated on top of the electrode surface, experimental data were compared to theoretical efficiencies and angular positions calculated using a code based on a rigorous coupled wave analysis (RCWA), which allows us modeling the optical response of the nanocrystalline titania gratings. This analytical method is typically applied to solve the scattering of wavelengths on the order of the features of a periodic nanostructure.[22] For the calculations, we assume that the patterned nanocrystalline TiO_2 has a refractive index n = 1.71 and that the height of the triangular grooves is 130 nm, which is the average value measured by AFM. As it can be seen in Figure 2B, there is fair agreement between theory (lines) and experiment (symbols), which evidences the good optical quality of the surface relief pattern.

The main idea behind patterning a grating in the TiO_2 surface is to increase the path length of photons within the sensitized electrode by effect of diffraction, regardless of the front or rear direction of incidence of incoming light. The light that reaches the patterned surface of the TiO_2 electrode is diffracted in different beams travelling in oblique directions. Hence, the residence time of diffracted photons through the photoanode

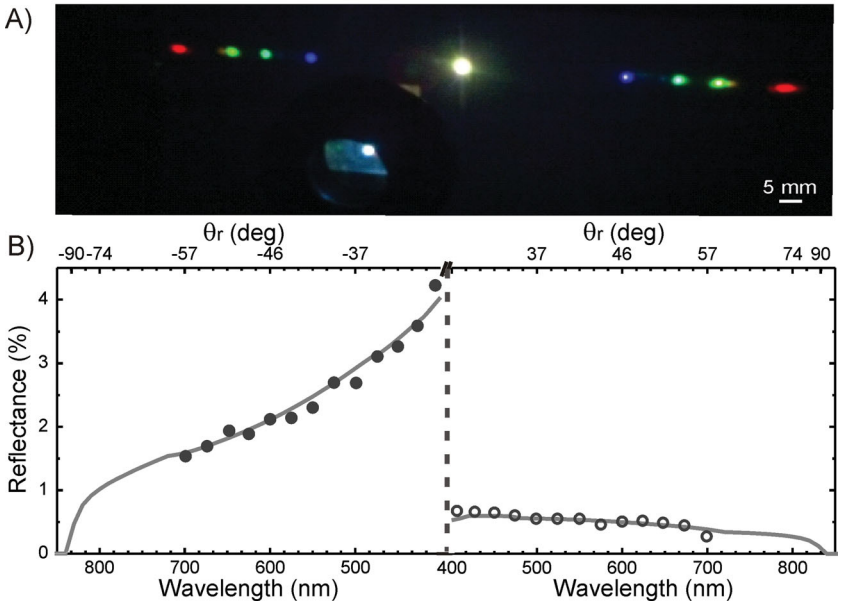

Figure 2. A) Photograph of diffraction pattern illuminating the electrode with four different wavelengths simultaneously. B) Theoretical (grey line) and experimental data (m = –1 black dots, m = 1 black open dots) of the spectral reflectance efficiency in air. The grating is assumed to be embedded between two media with refractive indexes 1.00 and 1.71.

is increased, which leads to increasing the absorption. This feature was confirmed for dyed nanocrystalline titania films of larger size (1 cm × 1 cm) and free of electrolyte, which allow us to characterize reliably total reflectance and transmittance in an integrating sphere in order to estimate the absorptance. Results are reported in **Figure 3**, with black and grey solid lines corresponding to patterned and flat dyed electrodes respectively. The absorptance of the nanopatterned electrode is larger than that of the flat one for both front and rear illumination, in good agreement with the fact that the surface relief works as a diffraction grating in both reflection and transmission modes. In order to compare with the effect on absorptance of a standard light harvesting enhancement method, a set of electrodes of the same area and thickness were coated with a thick (5 μm) layer of diffuse scattering particles employing a dispersion with a broad particle size distribution (150 nm to 250 nm). Typical results for these samples are also plotted in Figure 3 (gray dashed lines). As expected, the absorptance enhancement attained for these

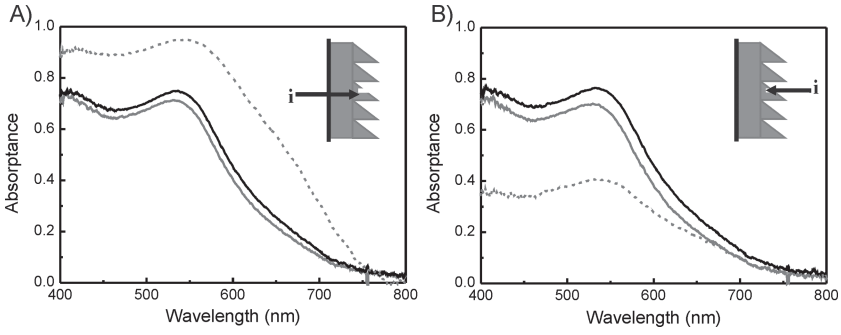

Figure 3. Absorptance curves measured from a flat TiO_2 film (grey line), a patterned TiO_2 film (black line) and a scattering layer coupled to the TiO_2 film (grey dashed line) after dye loading, measured under front (A) and rear (B) illumination.

electrodes is significantly larger than that attained for the patterned electrodes. However, under rear illumination the result is the opposite, patterned electrodes being considerably more efficient as absorbers than those containing diffuse scattering particles.

This effect was further confirmed with the results obtained for photovoltaic devices prepared with electrodes of similar design. **Figure 4** shows the photocurrent–voltage (IV) characteristics and the incident photon to collected electron (IPCE) efficiency spectra measured at normal incidence and front illumination from DSCs prepared using patterned (black solid lines) and unpatterned electrodes (grey lines), as well as an electrode coupled to a diffuse scattering layer (grey dashed line). Drawings at the top of Figure 4 schematize the diffraction modes that contribute to enlarging the light path within the patterned dye sensitized electrode in each case. In good agreement with the comparative analysis of absorptance, a scattering layer increased the cell performance under frontal illumination (left panel) but largely diminished its performance under back irradiation conditions (right panel); on the contrary, patterned TiO_2 photoanodes present systematically higher short circuit photocurrent (J_{sc}) than the reference ones under both frontal and rear illumination. In addition, the large enhancement observed at short frequencies in the IPCE plot for frontally illuminated cells, Figure 4C, agrees well with the calculations of the efficiencies of beams diffracted by such grating, as shown in Figure S1.B. Note that the spectral distribution of the IPCE is modified when the cell is illuminated from the counter electrode side, as it can be seen in Figure 4D, as the parasitic absorption of electrolyte, which is the incoming medium now, becomes more relevant at $\lambda < 500$ nm. Interestingly, if both contributions to the photocurrent are added, it can be seen that a DSC made with a patterned electrode presents a similar total photocurrent than one containing a diffuse scattering layer. This behaviour implies that a module based on the approach we are proposing would be more versatile for applications in which the cell illumination direction may vary from front to back, as it is typically the case for indoor applications.

These results demonstrate that the patterning of electrodes is a means to potentially achieve multidirectional improvement of the photocurrent. Actually, **Figure 5** displays the angular dependence of J_{sc} as extracted from the IV curves of cells tested for a wide range of incidence angles under both frontal and rear illumination conditions. In the experiments, unpolarized light is employed from a solar simulator impinging from either the electrode, Figure 5A, or the counter electrode, Figure 5B, sides, and with the incidence plane perpendicular (black solid line) or parallel (black dashed line) to the grooves

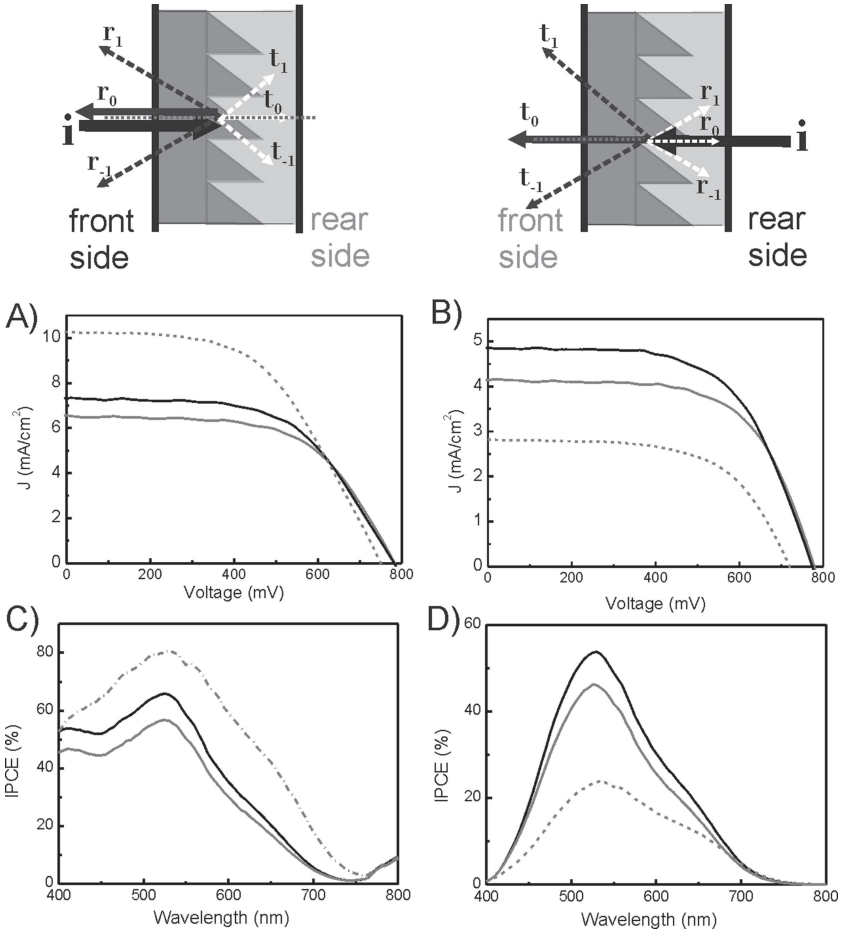

Figure 4. IV curves and incident photon to collected electron (IPCE) efficiencies measured from a reference cell (grey line), a cell integrating a patterned electrode (black line) and a cell containing a scattering layer coupled to the electrode (grey dashed line), measured under front (A and C) and rear (B and D) illumination.

in the grating, as illustrated in the scheme of Figure 5. For the sake of comparison, the response of cells containing flat electrodes and those same electrodes coupled to a diffuse scattering layer are plotted in solid and dashed grey lines, respectively. Results on patterned electrodes reveal an overall enhancement of the performance of the cell for a broad range of incoming light directions, for both front and rear illumination conditions. The values of J_{sc} vs incident angle show a cosine-like angular dependence. This behavior is a well-known effect resulting from the reduction of the apparent surface of the device when the incident angle increases.[23] On top of this effect, patterned electrodes show an enhancement of the photocurrent when the cell is tilted within a plane perpendicular to the grooves, and irradiated with an angle larger than 25°. This is likely a result of the partial trapping of the first diffracted order within the nanocrystalline titania film. The asymmetric section of the patterned grooves results in a larger photocurrent enhancement when the incoming light beam is inclined anticlockwise. This asymmetry further confirms that the origin of the observed enhancement is the longer trajectories of photons within the electrodes as a result of diffraction. As expected, it is only observed when the incidence plane is perpendicular to the channels.

A summary of all relevant cell parameters determined from the IV curves measured under frontal perpendicular illumination are summarized in Table S1. Remarkably, both open circuit photovoltage and fill factor remain unaltered, indicating that surface patterning has no deleterious effect on electron recombination and charge transport. Our results demonstrate that patterning of surface reliefs onto nanocrystalline titania electrodes is the first light harvesting strategy that allows improving the dye solar cell performance irrespective of the fact that light is coming from the front or the rear side and regardless of the angle of light incidence. Other approaches based on disordered or ordered scattering layers give rise to significant improvements under frontal illumination, but impedes rear light to reach the photoanode. Also, patterned surfaces, as it occurs for the case of photonic crystals, allow preserving the semitransparency of the cell.

3. Conclusions

The results herein presented are the first demonstration of a light harvesting enhancement strategy that allows improving the cell performance under both frontal and rear illumination conditions and for a broad range of angles of incidence in each case. This performance is achieved by patterning the surface of titania electrodes using a combination of soft-lithography and micro-stamping techniques. Both electron and force microscopy analyses confirmed the suitability of this method to attain high quality replicas of surface reliefs on the surface of TiO_2 nanocrystalline films, and the agreement between experimental and theoretical optical results demonstrate that such electrodes behave as high quality optical diffraction gratings. As the patterned surface diffracts incoming light both in reflection and transmission, its effect is to increase the light path of diffracted beams within the absorbing layer under both front and rear illumination conditions and regardless of the angle of incidence on each surface. The results herein presented constitute a proof of concept for a non-optimized relief design. This approach should be further explored under the guidance of theoretical design to find the surface relief patterns that yield the maximum enhancement of conversion efficiency for DSCs irrespective of the direction of the incoming light. This concept could be applied to modern buildings where design of functional glazing based on semi-transparent photovoltaic cells is needed.

4. Experimental Section

Preparation of Patterned Electrodes: Surface relief patterns were created on TiO_2 electrodes (4.5 micrometers thick, as measured in a profilemeter) by a combination of soft-lithography and micro-stamping,

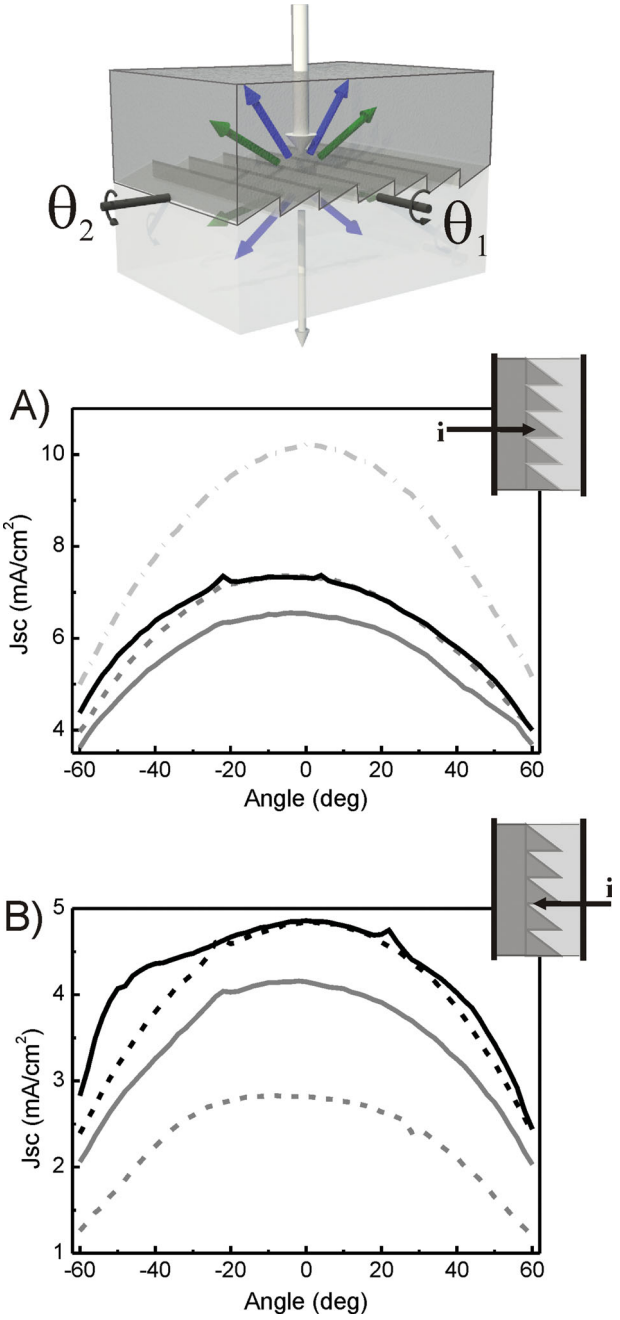

Figure 5. Scheme showing the two rotation axes used in the angular measurements. A) and B) show J_{sc} as a function of the incident angle of a cell integrating a patterned electrode measured as the cell is tilted around the rotation axis defined as θ_1 (black solid line) and θ_2 (black dashed line) under front (A) and rear illumination (B). Results of a similar characterization performed for a reference cell (grey solid line) and a cell including a scattering layer coupled to the electrode (grey dashed line) are also shown.

following a procedure thoroughly described by Whitesides et al.[24] First, polymer replicas of blazed one dimensional optical gratings (Edmund Optics Ruled Diffraction Grating #43–005) with a 833 nm period were obtained. The period of the grating (833 nm) was selected to yield diffraction effects at frequencies matching the absorption band of the dye that sensitized the porous electrode, i.e., a ruthenium based dye (N-719). First, we deposited a hard polydimethylsiloxane (h-PDMS) layer onto their surface, as this compound has been proven to reproduce with high fidelity a master surface pattern with nanometre scale features. After curing (60 °C, 30 min), a flexible soft PDMS layer was placed on top of the h-PDMS to ease handling and manipulation. Finally, a cured at 90 °C allows us obtaining an elastomeric film that can be used as a mould by putting it into conformal contact with a nanocrystalline titania paste (18-NRT, Dyesol) deposited onto a transparent conducting substrate. The TiO_2 paste was previously softened by heating at 60 °C during 15 min to facilitate the printing process and to prevent adhesion with the elastomer. Then, the molding process was performed by applying pressure between the titania film and the polymeric replica during 30 min, a heating step at 130 °C kept during the first 15 min followed by a cooling down to room temperature during the rest of the time. By doing this, high quality replicas of the stamp are produced without any damage, so it can be reused. After mechanical removal of the PDMS template, the nanocrystalline titania film was sintered at 500 °C to entirely remove the organic components of the paste. A scheme of the preparation procedure and an actual field-effect scanning electron microscopy (FESEM) picture of a moulded TiO_2 electrodes are displayed in Figure S2, where it can be clearly seen that, after the process is completed, the surface is shaped as a periodic arrangement of grooves.

Device Fabrication: Cleaned FTO glass substrates (TEC 11 Ω/cm^2, Nippon Sheet Glass) were soaked in 0.04 M $TiCl_4$ aqueous solution at 70 °C for 15 min, washed with distilled water, ethanol and dried at room temperature. After that, a TiO_2 paste (18-NRT, Dyesol) was coated onto these substrates by screen printing, resulting active layers with areas of 0.25 cm^2 and uniform thicknesses of 4.5 μm.

The sintered electrodes (patterned and flat reference) at 500 °C were soaked again into a 0.04 M $TiCl_4$ aqueous solution at 70 °C for 15 min and then washed with water and ethanol, and finally heated at 450 °C. To fabricate a 4.5 μm scattering layer coupled to the electrode, a paste containing TiO_2 large particles (WER2-O, Dyesol)was deposited via screen printing on top of the transparent electrodes. The scattering layers were subjected at 450 °C during 30 min.

All electrodes used in this work were carefully selected after checking their thickness and roughness using a motorized profilometer (Mahr-perthometer PGK), in order to establish an appropriate comparison.

The sensitization was carried out by dipping the TiO_2 electrodes overnight into a 0.2 mM in ethanolic solution of dye (N719, Solaronix), followed by rinsing in ethanol and dried. Counter-electrodes were made by deposition of colloidal platinum paste (Platisol T, Solaronix) onto a conductive FTO glass substrate and heating the ensemble at 400 °C for 10 min. The dyed TiO_2 electrodes were attached to the Pt counter electrode by using a thermo-polymer (Surlyn Meltonix 1170–25, Solaronix) as spacer between them. We used as electrolyte a solution of 100 mM I_2 (Aldrich, 99.999%), 100 mM LiI (Aldrich, 99.9%), 600 mM $[(C_4H_9)_4N]I$ (Aldrich, 98%), and 500 mM 4-tert-butylpyridine (Aldrich, 99%) in 3-methoxy propionitrile (Fluka, ≥99%). This solution was infiltrated into the sandwich structured cells by capillary force through two holes made previously at the back of the counter-electrode. Finally, both holes were sealed by Surlyn films and cover glasses.

Characterization: The patterned surface of the structures herein presented was characterized by atomic force microscopy (AFM) (Park Systems XE-100) working at tapping mode and by field-emission scanning electron microscopy (FESEM) (Hitachi S-4800 operating at 2 kV).

Diffraction efficiency was measured using an experimental setup mounted ad hoc on an optical bench and drawn in Figure S3. A supercontinuum white source (Fianium White Laser SC400) coupled to an acousto-optic tunable filter (Fianium AOTF-Dual) provides monochromatic incident radiation. Circularly polarized collimated light is shed onto the patterned electrode at normal incidence with respect to the substrate. Several spatial filters are placed between the source and the sample to obtain an approximately 1 mm^2 illumination spot on the sample surface. Angular resolution was determined by the size of the iris and its distance to a collimator lens that focus on an optical fiber that takes the collected light to a photodetector (Ocean Optics

USB2000+UV-VIS-ES). Measurements were performed between 400 and 700 nm, since it is the effective working range of the polarizing filter. Diffraction efficiency is given as the quotient between the intensity of a specific mode diffracted by the periodic structure and the intensity impinging directly on the detector from the light source.

The absorption properties of the different TiO_2 films were characterized using an experimental setup mounted on an optical bench, consisting of a halogen lamp (Lightsource HL 2000, Ocean Optics), an integrating sphere (Labsphere 10 inch) and a fiber coupled spectrometer (Ocean Optics USB2000+UV-VIS-ES).

Photovoltaic characterization of the cells was carried out with a solar simulator (Sun 2000, Abet Technologies) including a 150 W xenon arc lamp and the appropriate filter to replicate the AM1.5 solar spectrum. Intensity-voltage curves were obtained by applying an external bias to the cell and measuring the generated photocurrent with a digital source meter (Keithley 2400). Incident photon to collected electron (IPCE) efficiency measurements were acquired using an experimental setup composed of a 300 W xenon arc lamp, a monochromator with 1140 lines/mm grating (Model 272, Mcpherson) controlled by a digital scan drive system (Model 789A-3, Mcpherson) and a picoammeter (Keithley 6485). An UV filter with cut-off wavelength of 400 nm was used to remove second order harmonics exiting the monochromator. A silicon photodiode with calibration certificate (D8-Si-100 TO-8 Detector, Sphere Optics) was used to correct the cell response. To reduce spurious light reflections and refractions, which might lead to erroneous interpretations, all measurements were performed using a black mask covering the device.

The reproducibility and reliability of all results herein presented was confirmed by realizing several cells of each type and performing the same structural and photovoltaic characterization.

Supporting Information

Supporting Information is available from the Wiley Online Library or from the author.

Acknowledgements

The research leading to these results has received funding from the European Research Council under the European Union's Seventh Framework Programme (FP7/2007–2013)/ERC grant agreement n° 307081 (POLIGHT), the Spanish Ministry of Economy and Competitiveness under grants MAT2011–23593 and CONSOLIDER HOPE CSD2007–00007, and the Junta de Andalucía under grant FQM5247. The authors also thank CITIUS for help with AFM and FESEM characterization.

Received: April 10, 2014
Revised: May 23, 2014
Published online: June 16, 2014

[1] B. O'Regan, M. Grätzel, *Nature* **1991**, *353*, 737.
[2] M. K. Nazeeruddin, A. Kay, I. Rodicio, R. Humphry-Baker, E. Müller, P. Liska, N. Vlachopoulos, M. Grätzel, *J. Am. Chem. Soc.* **1993**, *115*, 6382.
[3] D. Zhou, R. Biswas, *J. Appl. Phys.* **2008**, *103*, 093102.
[4] P. Bermel, C. Luo, L. Zeng, L. C. Kimerling, J. D. Joannopoulos, *Opt. Express* **2007**, *15*, 16986.
[5] L. Zheng, P. Bermel, Y. Yi, B. A. Alamariu, K. A. Broderick, J. Liu, C. Hong, X. Duan, J. Joannopoulos, L. C. Kimerling, *Appl. Phys. Let.* **2008**, *93*, 221105.
[6] K. R. Catchpole, A. Polman, *Opt. Express* **2008**, *16*, 21793.
[7] A. Atwater, A. Polman, *Nat. Mater.* **2010**, *9*, 205.
[8] A. Usami, *Chem. Phys. Lett.* **1997**, *277*, 105.
[9] S. Hore, C. Vetter, R. Kern, H. Smit, A. Hinsch, *Sol. Energy Mater. Sol. Cells* **2006**, *90*, 1176.
[10] F. E. Gálvez, E. Kemppainen, H. Míguez, J. Halme, *J. Phys. Chem.* **2012**, *116*, 11426.
[11] L. I. Halaoui, N. M. Abrams, T. E. Mallouk, *J. Phys. Chem. B* **2005**, *109*, 6334.
[12] S. Colodrero, A. Mihi, L. Häggman, M. Ocaña, G. Boschloo, A. Hagfeldt, H. Míguez, *Adv. Mater.* **2009**, *21*, 764.
[13] N. Tetreault, M. Grätzel, *Energy Environ. Sci.* **2012**, *5*, 8506.
[14] S. Colodrero, A. Forneli, C. López-López, L. Pellejà, H. Míguez, E. Palomares, *Adv. Funct. Mater.* **2012**, *22*, 1303.
[15] A. Mihi, H. Míguez, *J. Phys. Chem. B* **2005**, *109*, 15968.
[16] G. Lozano, S. Colodrero, O. Caulier, M. E. Calvo, H. Míguez, *J. Phys. Chem. C* **2010**, *114*, 3681.
[17] J. Kim, J. K. Koh, B. Kim, J. H. Kim, E. Kim, *Angew. Chem. Int. Ed.* **2012**, *51*, 6864.
[18] S. Wooh, H. Yoon, J. H. Jung, Y. G. Lee, J. H. Koh, B. Lee, Y. S. Kang, K. Char, *Adv. Mater.* **2013**, *25*, 3111.
[19] D. Barettin, A. Di Carlo, R. De Angelis, M. Casalboni, P. Prosposito, *Opt. Express* **2012**, *20*, 889.
[20] J. Lee, M. Lee, *Adv. Energy Mater.* **2014**, *4*.
[21] C. Palmer, E. Lowen, *Diffraction Grating Handbook*, Richardson Grating Laboratory, Rochester, NY **2002**.
[22] M. G. Moharam, T. K. Gaylord, *J. Opt. Soc. Am.* **1981**, *71*, 811.
[23] C. López-López, S. Colodrero, M. E. Calvo, H. Míguez, *Energy Environ. Sci.* **2013**, *6*, 1260.
[24] D. Qin, Y. Xia, G. M. Whitesides, *Nat. Protoc.* **2010**, *5*, 491.